Front. Chem. Sci. Eng. 2022, 16(9): 1399−1406
https://doi.org/10.1007/s11705-022-2149-z

COMMUNICATION

Chemically triggered life control of “smart” hydrogels through click and declick reactions

Xing Feng[1], **Meiqing Du**[1], **Hongbei Wei**[1], **Xiaoxiao Ruan**[1], **Tao Fu**[1], **Jie Zhang** (✉)[2], **Xiaolong Sun** (✉)[1]

1 Key Laboratory of Biomedical Information Engineering of Ministry of Education, School of Life Science and Technology, Xi’an Jiaotong University, Xi’an 710049, China
2 The Fourth Military Medical University, Xi’an 710032, China

Abstract The degradation of polymeric materials is recognized as one of the goals to be fulfilled for the sustainable economy. In this study, a novel methodology was presented to synthesize multiple highly cross-linked polymers (i.e., hydrogels) through amine–thiol scrambling under mild conditions. Amine-terminated poly(ethylene glycol) (PEG-NH_2) was reacted with the representative conjugate acceptors to synthesize hydrogels in organic and aqueous solutions, respectively. The materials above exhibited high water-swelling properties, distributed porous structures, as well as prominent mechanical strengths. It is noteworthy that the mentioned hydrogels could be degraded efficiently in hours to release the original coupling partner, which were induced by ethylene diamine at ambient temperature through amine-amine metathesis. The recovered PEG-NH_2 reagent could be employed again to regenerate hydrogels. Due to the multiple architectures and functions in polymeric synthesis, degradation and regeneration, a new generation of “smart” materials is revealed.

Keywords hydrogels, degradation, synthesis, regeneration

1 Introduction

Highly cross linked soft materials (e.g., hydrogels) turn out to be an ideal material and has been extensively employed in various fields for their high water absorption, programmability, good biocompatibility, easy operation and tunable mechanical properties [1]. For instance, hydrogels have achieved wide applications in bioprinting [2], bio-inking [3], tissue engineering [4,5], regenerative medicine [6], drug delivery [7], biosensing [8], etc. Moreover, as economic society is leaping forward, and sustainable development is being continuously promoted, hydrogels are serving as a powerful tool in sustainable energy, water purification [9], maximum energy efficiency [10], optical component [11], molecular testing [12], wearable device [13], actuators [14,15], etc. Furthermore, worn-out sensors will primarily end up as electronic waste, thereby probably polluting the environment and endangering human health [16].

On the whole, the natural hydrogels (e.g., hyaluronic acid, collagen and alginate) are degradable, whereas they commonly face the limitations of unique spatial divisions and variable time scale involved in manipulating immune response or moderate mechanical properties [17,18]. In addition, the synthetic hydrogels (e.g., poly(acrylicacid) (PAA), poly(vinyl alcohol) (PVA) and PEG) exhibiting adjustable mechanical properties break through the limitations, so considerable hydrogels exhibiting high mechanical strength have been developed [19]. Though extensive studies have been conducted on degradable materials, most of the materials above are based on polymers (e.g., PVA, polyacrylamide [20], chitosan [21], PAA [22], poly (acrylic acid) [23]). Substantial synthetic materials cannot be degraded, remolded, or reformed, thereby triggering several adverse consequences (e.g., pollutions, processing and manufacturing difficulties and energy-waste). On the whole, synthetic PEGs are costly, thereby limiting their wide applications and large-scale preparation. For this reason, the PEG reagents should be recycled from the existing or finished products and reused. To the best of our knowledge, however, the recovering work on PEG-based hydrogels has been rarely investigated. Thus, such a type of novel materials exhibiting degradable properties should be produced in the field of material, which can achieve a wide range of applications (e.g., medicine and drug delivery to microelectronics and environmental protection) [24,25].

Received September 8, 2021; accepted December 7, 2021

E-mails: zhangjie78@fmmu.edu.cn (Zhang J.), x.l.sun86@xjtu.edu.cn (Sun X.)

2 Experimental

2.1 Synthesis of conjugate acceptors (**CA**s)

Meldrum's acid derived cross-linker **1** and barbituric acid derived cross-linker **3** were synthesized by complying with the previous procedures presented by Wentrup [26] and Sheikha [27], respectively. In addition, the cross-linker **2** was synthesized in accordance with the reported work by Kalow [28]. Chemicals originated from TCI Chemicals, Aladdin Chemicals and other reagent manufacturers.

2.2 Preparation of hydrogels

CAs and 4-PEG amine ($M_n \approx 10$ kDa) were dissolved in acetonitrile or deionized water (10% acetonitrile as co-solvent) and then swirled at ambient temperature. The solution was moved to a mold exhibiting a diameter of 25 mm and a thickness of 1 mm for the gelation of the solution. The hydrogels were dried and then swelled in PBS buffer for six hours until the equilibrium was reached for all tests. The hydrogel samples applied for rheological testing reached the swelling equilibrium.

2.3 Characterizations of hydrogels

Rheological measurements were performed by applying a Rheometer (MCR 302, Anton Paar) equipped with a parallel plate geometry (25 mm rotor). Scanning electron microscopy (SEM) images were captured under ultra-high resolution field emission scanning electron microscope (Tescan Maia3 LMH, Czech Republic). All mechanical tests were performed with the use of an electronic universal testing machine (UTM2203, SUNS, China) equipped with 100N load cell, and the temperature fluctuation in the test was reported to be lower than 2 °C·h^{-1} to eliminate the effect of temperature fluctuations on hydrogel testing. The hydrogel samples were characterized under Raman spectrometer (Horiba Jobin-Yvon, LabRam Aramis Raman Spectrometer, France) with 532 nm excitation wavelength. The pH (potential-of-hydrogen) was measured by employing an instrument equipped with FE28-Meter (FiveEasy Plus, METTLER TOLEDO).

2.4 Degradation and regeneration of hydrogels

The fully swollen hydrogel was transferred to the ethylenediamine solution for degradation. After the degradation, the mixture was collected, and the mixed solution underwent the rotary evaporation to remove ethylenediamine. Moreover, a white solid was produced and dried in vacuum. Subsequently, the minimal amount of chloroform was exploited to dissolve the solid matter, and the mixed solution was poured into ice ether for low-temperature centrifugation to produce a white precipitate, which was then dried in vacuum to produce the recovered 4-PEG amine. Next, the solution was dried in vacuum to produce a white powder 4-PEG amine. 4-PEG amine was confirmed through NMR spectrum in $CDCl_3$.

3 Results and discussion

CAs (**1**, **2**, **3**) with similar structures are all containing adjacent bis-methylthiol esters which can be scrambled by amine derivatives [29,30]. Thus, 4-PEG amine **4** was employed to react with the representative **CA**s in organic and aqueous mediums, respectively, to produce hydrogels (Fig. 1). The properties of the materials above made from different acceptors in the two solvents were characterized and compared. It is noteworthy that all the hydrogels could be degraded quantitatively in hours by adding ethylene diamine (EDA) through amine–amine metathesis [31,32]. Through the decoupling reactions between bis-vinylogous amide **CA**s and EDA, the networks were cleaved to release the original coupling partners (Fig. 1). Moreover, the 4-PEG amine was recovered through dialysis and precipitation, which was subsequently verified by nuclear magnetic resonance (NMR) and gel penetration chromatography (GPC). Furthermore, the recovered monomer was employed again to effectively regenerate soft materials. New hydrogel materials were successfully synthesized, further succeeded in monomer recovering after degradation to regenerate hydrogels. The recoverable polymers based on dynamic covalent bonding refer to a type of new environmentally "intelligent" materials.

First, hydrogels (A-1, A-2 and A-3) were synthesized in organic solvent, i.e., acetonitrile due to the rapid amine-thiol scrambling (Fig. 2). Two equivalents of **CA**s were mixed with one equivalent 4-PEG amine ($M_n \approx 10$ kDa) (Figs. S1–S3, cf. Electronic Supplementary Material, ESM). Through the vortex processing, monomers **2**, **3** were cross-linked with 4-PEG amine to generate the matrixes of A-2 and A-3, respectively, in 5 min through amine–thiol scrambled and methyl mercaptan released (Fig. 2(a)). Besides, an overlong time of 27 min was required to form A-1, which indicated a slow coupling speed due to the different leaving abilities exhibited by methanethiol on **CA**s. The swelling ratios in water for the hydrogels reached 5.7, 4.5 and 5.9, respectively, from the measured sizes (Fig. 2(b)). The materials were observed to be stable and hardly hydrolyzed in water over 15 d (Fig. S4, cf. ESM). Furthermore, as indicated from the results of rheological analysis, the hydrogel maintained the properties of an elastomer in an hour, which demonstrated the stability of the soft materials (Fig. S5, cf. ESM). SEM was performed to present the microstructure of the materials made from different **CA**s (Figs. 2(c), S6–S8, cf. ESM). Figure 2(c) illustrates the typical SEM images of the cross sections of A-1, -2 and -3 with magnification (M) = 15 k. Under the difference in cross linkers, A-2 showed a larger pore size (5 μm) than A-1/A-3

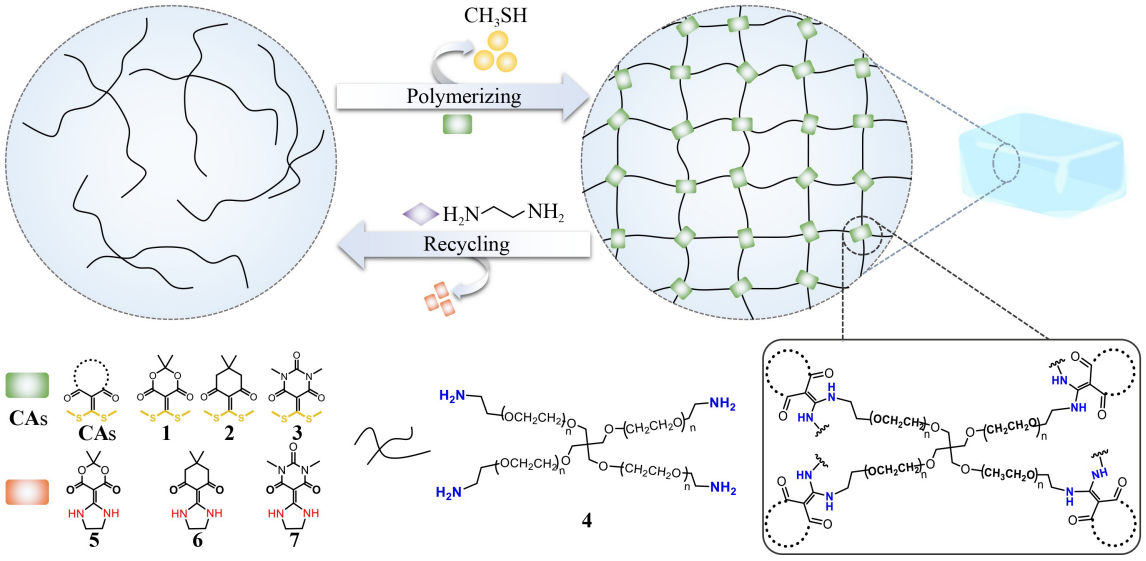

Fig. 1 Recycling of soft materials through "amine–thiol coupling and amine–amine decoupling" reactions: materials of synthesis through the reactions between **CAs 1**, **2**, **3** and 4-PEG amine **4** with releasing methyl mercaptan (CH_3SH); EDA-induced decoupling to release the original amine partner **4** and five-membered ring product **5**, **6**, **7**. The recyclable monomer was employed again to regenerate soft materials.

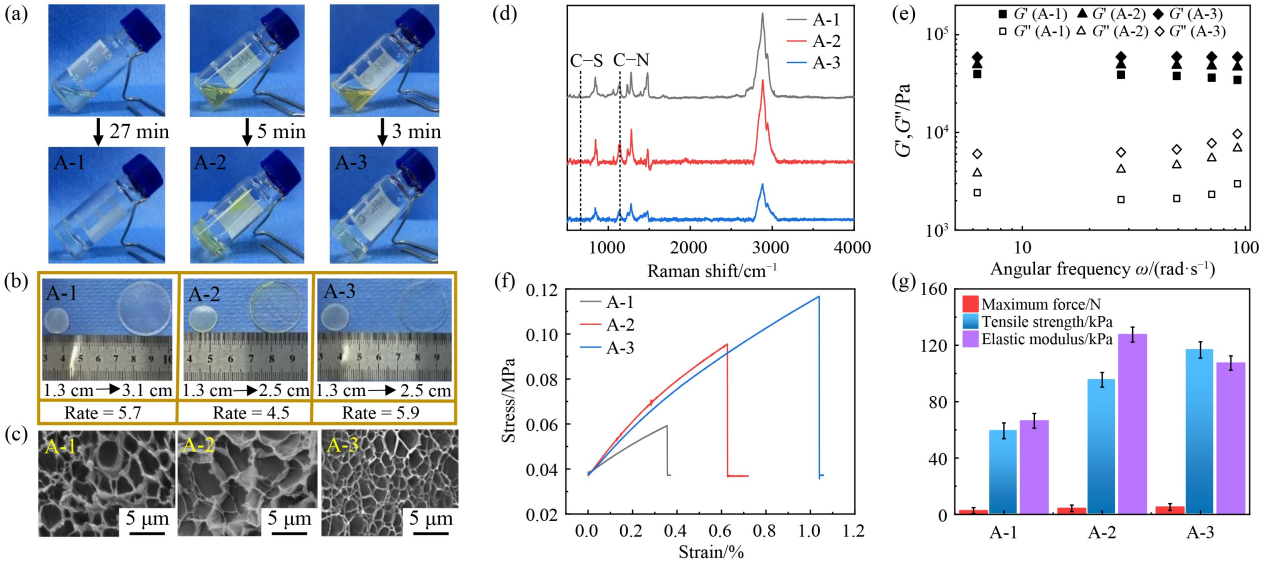

Fig. 2 (a) Formation of A-1, -2, -3 in acetonitrile; (b) Swelling properties for A-1, -2, -3 in water, size changes and swelling ratios; (c) SEM images for A-1, -2, -3. M = 15 k; (d) Raman spectra for A-1, -2, -3; (e) Storage modulus (G') and loss modulus (G'') for swelled A-1, -2, -3; (f) Stress-strain tension test for swelled A-1, -2, -3; (g) Maximum force, tensile strength and elastic modulus test for swelled A-1, -2, -3.

(2.0–3.0 μm). Furthermore, to examine the chemical structure of A-1, -2 and -3, the bonds were characterized by Raman spectroscopy to determine the occurrence of amine–thiol substitution (Figs. S9–S11, cf. ESM). The stretching vibration peak of the C–S bonds at 712 cm^{-1} from the monomers vanished, while the peak of the C–N bonds at 1135 cm^{-1} appeared, which demonstrated the amine–thiol scrambling (Fig. 2(d)). Next, the mechanical property exhibited by hydrogels was consistent with rheological data. Figure 2(e) presents the variations of storage modulus (G') and loss modulus (G'') of swelled hydrogels under the fixed frequency (1 to 150 $rad \cdot s^{-1}$). Overall, the materials were mainly elastically deformed with $G' > G''$ under the entire frequency range, thereby indicating the essence of elastic solids. The G' values of the gels complied with the order: A-3 (~ 56 kPa) > A-2 (~ 40 kPa) > A-1 (~ 38 kPa) at this range of angular frequencies, which means that the A-3 were more robust than A-2/A-1 in resistance to shear. In kinetics from rheometry, the G' for all the hydrogels were constant at 48 k (A-1), 46 k (A-2) and 61 k (A-3), respectively, over 300 s, thereby verifying the property of the robust elastomers (Fig. S12, cf. ESM). Next, the tensile properties of these soft materials were tested. Figure 2(f) plots the

tensile stress-strain curves of A-1, -2 and -3 samples after the swelling. According to the figure above, A-1 exhibited an extremely low tensile strength (59.3 kPa), whereas A-3 could withstand greater strain (～1.06%), which demonstrated its higher crosslink density. In addition, Figure 2(g) presents the maximum force, tensile strength and elastic modulus of A-1, -2 and -3. In comparison, A-2 achieved the greatest elastic modulus of 130 kPa, while A-3 achieved the largest tensile strength of 120 kPa. Thus, A-2 was proved to be the least prone to deformation. Since the crosslinking density has been found as a pivotal factor of the strength of the hydrogel, different ratios between acceptor **3** and 4-arm PEG amine were adopted to verify whether the tensile properties of the materials would be inconsistent. With the decrease in the proportion of conjugated receptors in the reaction system, the material could withstand greater strain (from 1.0% to 3.0%) and its brittleness was reduced, accompanied by a reduction in the stress that could be tolerated (from 0.8 MPa to 0.5 MPa) (Fig. S13, cf. ESM).

Water, the most abundant of resources worldwide, has been found as an ideal medium for chemical reactions. Inspired by this finding, this study attempted to synthesize the soft materials by replacing organic solvent with water (Fig. 3). Accordingly, monomers **1**, **2**, **3** (2 equiv.) were mixed with 4-PEG amine (1 equiv. $M_n \approx 10$ kDa) in deionized water (10% acetonitrile as co-solvent), respectively (Figs. S14–S16, cf. ESM). The cross linking and formation of hydrogels W-1, -2 and -3 were slower and required 30, 63 and 51 h, respectively, which were inconsistent with the performances in organic solvent. This was most probably due to the reduced electrophilicity of conjugate acceptors once linked with an amine, as well as the reduced mobility and interaction between molecules with the increase in the viscosity during the gel formation. Moreover, as opposed to the reaction speed in aprotic acetonitrile, the speed was **1** > **3** > **2** under protic aqueous condition for the gelation (Fig. 3(a)). In predication, the pH impacted the coupling reactions, so the pH of the solutions was then tested. According to Fig. S17 (cf. ESM), the water system was weakly alkaline (～8.6) in the synthetic process, thereby accelerating the amine-thiol substituting on two sides of the conjugate acceptors [33].

When the amine–thiol replacement is identified in water, the reduced scrambling points will reduce the crosslinking density as predicted above. In this study, the mechanical properties of the mentioned materials would be reduced (Figs. S18 and S19, cf. ESM). First, aqueous swelling ratios of the three hydrogels were 6.2, 6.8, 7.5, respectively (Fig. 3(b)), higher than those made from acetonitrile (Figs. S20 and S21, cf. ESM). In SEM, the pore size of W-2 reached the largest (～6 μm), while W-1 and W-3 approached 4 μm (Figs. 3(c), S22–S24 (cf. ESM)). The pore sizes of W-1, -2 and -3 are generally larger than that of A-1, -2 and -3. This phenomenon could be explained by the hypothesis that in the water system, more unilateral amine–thiol replacement occurred on **CA**s, thereby causing a decrease in the cross-linking density. In Raman spectra, the results demonstrated the crosslinking formation in W-1, -2 and -3 matrixes, the stretching vibration peak appeared at 1135 cm^{-1} for C–N bond along with the decrease of the peak of C–S groups at 712 cm^{-1} (Fig. 3(d)). In rheometry, the G' value of the gels generally decreased, which complied with the order: W-3 (～48 kPa) > W-2 (～32 kPa) > W-1 (～28 kPa) at the monitored angular frequency. In kinetics, the G' values for the hydrogels reached 23 kPa (W-1), 34 kPa

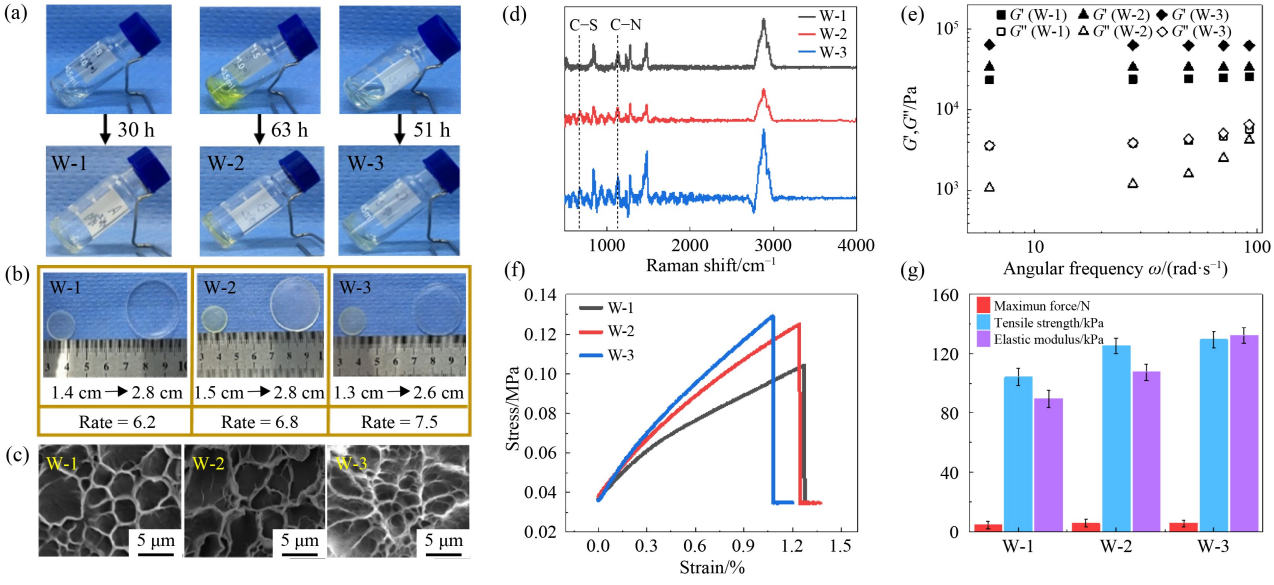

Fig. 3 (a) Hydrogel formation for W-1, -2, -3 in water (10% acetonitrile as co-solvent) over time; (b) Swelling properties of W-1, -2 and -3 in water, size changes and swelling ratios; (c) SEM images of W-1, -2 and -3 after the swelling and the lyophilization. $M = 15$ k; (d) Raman spectra for W-1, -2 and -3; (e) Storage modulus (G') and loss modulus (G'') for W-1, -2 and -3 after the swelling; (f) Stress-strain tension test for W-1, -2 and -3 after the swelling; (g) Maximal force, tensile strength and elastic modulus test for the swelled samples of W-1, -2 and 3.

(W-2), 62 kPa (W-3), respectively, over 300 s (Fig. 3(e), Fig. S18).

In comparison, the hydrogels prepared from the two different systems exhibited different properties, as listed in Table 1. Interestingly, it can be observed that stress-strain trends for W-1, -2 and -3 were opposite to the order of the materials of A-1, -2 and -3 (Fig. 2(f) and Fig. 3(f)). To be specific, A-3 made from the organic system exhibited a stronger strain, whereas the strain range of W-3 was the smallest in the water system. It was noteworthy that the strain range of the hydrogels made from water was larger than those made from acetonitrile. The elastic modulus and tensile strength of W-3 reached 130 kPa. Moreover, the elastic modulus and tensile strength increased by nearly 40 kPa from A-1 to W-1 (Fig. 3(f) and Fig. 3(g)). Accordingly, the mechanical properties of hydrogel synthesized from the organic system were found to be better than those from water (Table 1). Subsequently, the crosslinking densities for all the hydrogels were calculated to explain the mechanical properties (Table 1). The densities of W-1, -2 and -3 were lower in general meaning of reduced crosslinking than the hydrogels made from acetonitrile. In the aprotic solvent, the scrambling reaction of amine–thiol was more likely to occur, whereas the nucleophilicity of amine was weakened in water.

From perspective of environmental protection and energy conservation, degradation of polymeric materials into non-toxic small molecules or started monomers would be highly valued. To realize degradation of synthetic materials, stimuli-responsive dynamic covalent bonding would be a powerful tool. Subsequently, the degradation properties of all the hydrogels were examined through amine-amine metathesis induced by EDA (Fig. 4). The swelled A-1, -2 and -3/W-1, -2 and -3 samples were processed in EDA and tracked by time (Fig. 4(a)). The initial solid

Table 1 Comparison of hydrogels properties

Property	A-1	A-2	A-3	W-1	W-2	W-3
Gelation time	27 min	5 min	3 min	30 h	63 h	51 h
Swelling ratio	5.7	4.5	4.9	6.2	6.8	7.5
Pore size/μm	2–3	5	2–3	3–4	6	3–4
Storage modulus/kPa	48	46	61	23	34	48
Tensile strength/kPa	59.3	95.5	116.7	104.2	125.2	129.3
Elastic modulus/kPa	66.4	127.6	107.4	89.3	107.4	132.1
Crosslinking density	18.62	17.85	23.67	8.92	13.19	18.62

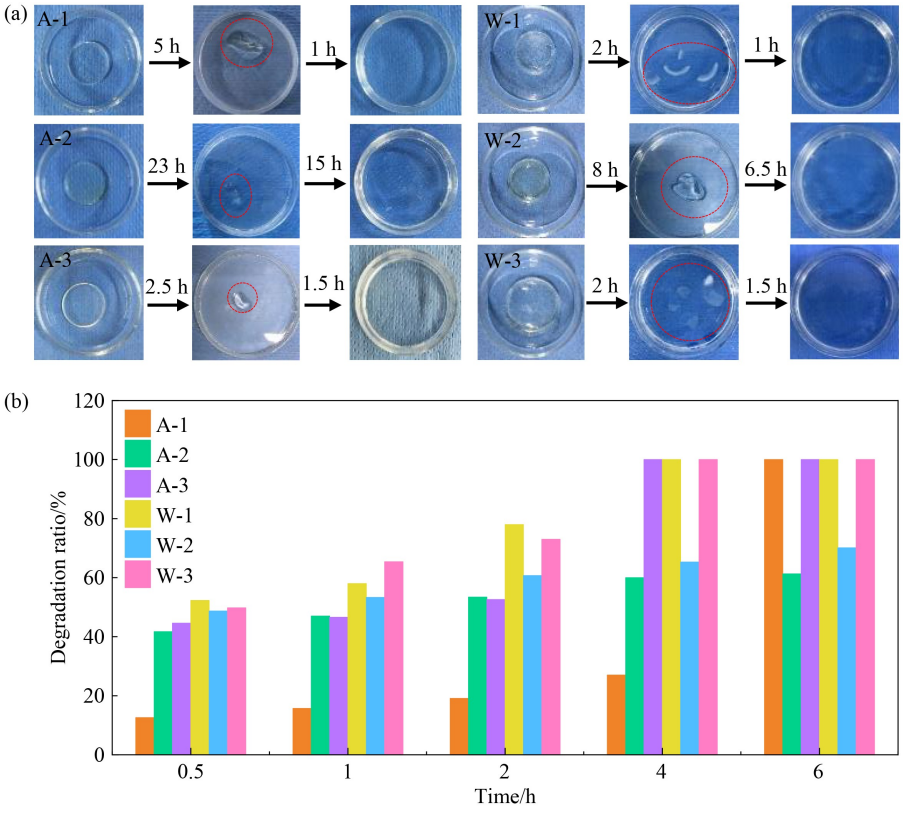

Fig. 4 (a) Degradation of all materials by EDA (Initial status of materials (left dishes); residue of materials after degradation for a certain amount of time (middle dishes); clear solutions after complete degradation (right dishes)); (b) Kinetics of degradation for all materials in EDA through measuring weight.

samples displayed round and intact status. Moreover, the weight of the hydrogels was measured and recorded in a time-dependent manner. Impacted by the distinctive structures on the **CA**s and degree of crosslinking, the degradation speed achieved the order of A-3 > A-1 > A-2, while A-2 was significantly resistant to degradation with requirement of 38 h. In comparison, hydrogels (W-1, -2 and -3) made from water showed faster speed in decomposition by EDA. According to Fig. 4(a), 3, 14.5 and 3.5 h were required for samples W-1, -2 and -3, respectively, to prepare clear solutions cleaved by EDA. Likewise, W-2 made from monomer **2** was found to be more difficult to be degraded than W-1 and W-3 under the identical condition (Fig. 4(b)). As described above, all the soft materials could be degraded by ethylene diamine for the potential recycling of 4-PEG amine (see below), which demonstrated the occurrences of amine-amine metathesis between bis-vinylogous amide on conjugate acceptors and amines on EDA.

Next, the original coupled partners were recovered after new hydrogels were degraded and regenerated by exploiting recycled reagent and monomers **1**, **2**, **3** (Fig. 5). The degraded samples processed by EDA were mixed together and then dried under vacuum. Afterwards, the residues were dissolved in the minimum amount of chloroform and precipitated from cold ether to prepare white fine powders (inset pictures in Fig. 5(a)). The recovered ratio of the 4-PEG amine was approximately 60% on average in three tests. Subsequently, ^{1}H NMR spectra confirmed that the proton peaks for the recovered product were consistent with those of the commercial reagent in $CDCl_3$ (Fig. 5(a)). Furthermore, molecular weight and retention time for the recovered and started 4-PEG amine were analyzed through GPC, which resulted in over-lapped peaks at the identical retention time of 8.5 min (Fig. 5(b)).

Reactivity of the recovered monomer should be studied and investigated in depth. Thus, utilizing the reagent (1 equiv.) to react with the same **CA**s (2 equiv.), new hydrogels ReA-1, 2, 3 were formed in acetonitrile (Fig. 5(c)). To examine the mechanical properties of the newly synthesized materials, rheological analysis was conducted (Figs. 5(c), S25 (cf. ESM) and Table 2). The *G*' of the novel materials decreased from the original values of 56 kPa/61 kPa/47 kPa (A-1/A-2/A-3) to 10 kPa/15 kPa/25 kPa (ReA-1/ ReA-2/ReA-3), respectively. In addition, their tensile properties were reduced, as compared with those made from original 4-PEG amine. According to Figs. S26-S27 (cf. ESM), the tensile strength and elastic modulus of ReA-1 decreased from (59.3 kPa, 21.7 kPa) to (66.4 kPa, 38.3 kPa), and those of ReA-2 (40.1 kPa, 63.2 kPa) declined to half of the original values (95.5 kPa,

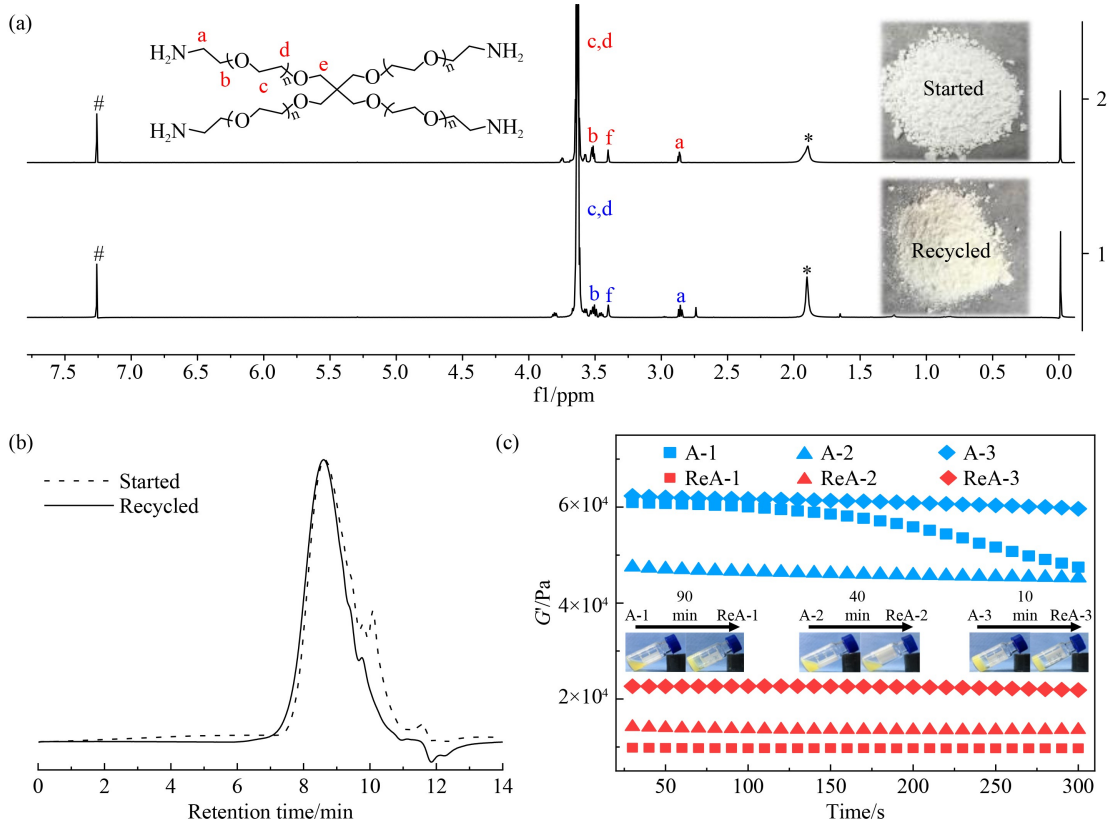

Fig. 5 (a) Proton NMR for started and recycled 4-PEG amine in $CDCl_3$; (b) GPC for started and recycled 4-PEG amine in DMF; (c) Storage modulus (*G*') and loss modulus (*G*") for ReA-1, -2, -3 after the swelling in the mode of time scan. Inset photos: regeneration of materials by using recycled 4-PEG amine in acetonitrile.

Table 2 Comparison of properties of A-1, -2, -3 and ReA-1, -2, -3

Property	A-1	A-2	A-3	ReA-1	ReA-2	ReA-3
Gelation time	27 min	5 min	3 min	90 min	40 min	10 min
Storage modulus/kPa	48	46	61	9.8	14	84.3
Tensile strength/kPa	59.3	95.5	116.7	21.7	40.1	83.9
Elastic modulus/kPa	66.4	127.6	107.4	38.3	63.2	84.3
Crosslinking density	18.62	17.85	23.67	3.8	5.43	8.54

127.6 kPa), while the tensile properties of ReA-3 (83.9 kPa, 84.3 kPa) were kept approximately at 75% of the original values (116.7 kPa, 107.4 kPa). The reduced crosslinking densities calculated in Table 2 for the re-synthesized materials led to the sacrificed mechanical properties. Besides, the recycling process was repeated for three times (recovery ratio kept at 60%) for A-3, and each time the recycled 4-PEG amine could be well gelled with the **CA**s (Fig. S28, cf. ESM). The reduced performances above could be explained by the reduced reactivity of the recovered 4-PEG amine from incomplete degradation, not exactly as the purchased one. Fortunately, their stabilities were kept, which showed their promising further applications.

4 Conclusions

In brief, polymeric materials were degraded through amine–thiol "clicking" and amine-amine "declicking" via conjugate acceptors. Commercially available PEG-NH_2 was clicked with three representative conjugate acceptors to develop soft materials under mild conditions through amine–thiol scrambling. The reaction and formation of materials were successfully operated in solvents of acetonitrile and water, respectively. Next, the materials above achieved high water swelling ratios of 7.5, distributed pore sizes from 2 to 6 μm and high mechanical strengths with G' of 56 kPa, which were found with extensive potential applications. More importantly, all the soft materials can be degraded efficiently in hours to release the started coupling partner, which were induced by ethylene diamine through chemically triggered amine-amine metathesis. 4-PEG amine achieved a recovery rate of 60%, and it could be employed to regenerate soft materials. Compared with the reported research on hydrogel recovery [34], this study degraded and recovered the raw started material and further examined the properties and recycling efficiency. Due to the multiple architectures and functions in polymeric synthesis, degradation and regeneration through dynamic covalent bonding, a new generation of materials with promising applications is revealed.

Electronic Supplementary Material Supplementary material is available in the online version of this article at https://dx.doi.org/10.1007/s11705-022-2149-z and is accessible for authorized users.

References

1. Liu X, Liu J, Lin S, Zhao X. Hydrogel machines. Materials Today, 2020, 36(25): 102–124
2. Hockaday L A, Kang K H, Colangelo N W, Cheung P Y, Duan B, Malone E, Wu J, Girardi L N, Bonassar L J, Lipson H, et al. Rapid 3D printing of anatomically accurate and mechanically heterogeneous aortic valve hydrogel scaffolds. Biofabrication, 2012, 4(3): 035005–035017
3. Buwalda S J, Boere K W, Dijkstra P J, Feijen J, Vermonden T, Hennink W E. Hydrogels in a historical perspective: from simple networks to smart materials. Journal of Controlled Release, 2014, 190(21): 254–273
4. Perez-San Vicente A, Peroglio M, Ernst M, Casuso P, Loinaz I, Grande H J, Alini M, Eglin D, Dupin D. Self-healing dynamic hydrogel as injectable shock-absorbing artificial nucleus pulposus. Biomacromolecules, 2017, 18(8): 2360–2370
5. Cheng H, Yue K, Kazemzadeh-Narbat M, Liu Y, Khalilpour A, Li B, Zhang Y S, Annabi N, Khademhosseini A. Mussel-inspired multifunctional hydrogel coating for prevention of infections and enhanced osteogenesis. ACS Applied Materials & Interfaces, 2017, 9(13): 11428–11439
6. Zhao X, Wu H, Guo B, Dong R, Qiu Y, Ma P X. Antibacterial anti-oxidant electroactive injectable hydrogel as self-healing wound dressing with hemostasis and adhesiveness for cutaneous wound healing. Biomaterials, 2017, 122(4): 34–47
7. Li J, Mooney D J. Designing hydrogels for controlled drug delivery. Nature Reviews Materials, 2016, 1(12): 1–17
8. Choi M, Choi J W, Kim S, Nizamoglu S, Hahn S K, Yun S H. Light-guiding hydrogels for cell-based sensing and optogenetic synthesis *in vivo*. Nature Photonics, 2013, 7(12): 987–994
9. Xu L, Chen K, Chen G Q, Kentish S E, Li G. Development of barium@alginate adsorbents for sulfate removal in lithium refining. Frontiers of Chemical Science and Engineering, 2020, 15(1): 198–207
10. Huang Y, Li H, He X, Yang X, Li L, Liu S, Zou Z, Wang K, Liu J. Near-infrared photothermal release of hydrogen sulfide from nanocomposite hydrogels for anti-inflammation applications. Chinese Chemical Letters, 2020, 31(3): 787–791
11. Guo Y, Bae J, Fang Z, Li P, Zhao F, Yu G. Hydrogels and hydrogel-derived materials for energy and water sustainability. Chemical Reviews, 2020, 120(15): 7642–7707
12. Choi M, Humar M, Kim S, Yun S H. Step-index optical fiber made of biocompatible hydrogels. Advanced Materials, 2015, 27(17): 4081–4086
13. Yan D, Liu S, Jia Y G, Mo L, Qi D, Wang J, Chen Y, Ren L. Responsive polypseudorotaxane hydrogels triggered by a

compatible stimulus of CO_2. Macromolecular Chemistry and Physics, 2019, 220(12): 1900071–1900076

14. Chalmers E, Li Y, Liu X. Molecular tailoring to improve polypyrrole hydrogels' stiffness and electrochemical energy storage capacity. Frontiers of Chemical Science and Engineering, 2019, 13(4): 684–694
15. Yang C, Suo Z. Hydrogel ionotronics. Nature Reviews Materials, 2018, 3(6): 125–142
16. Arslan H, Nojoomi A, Jeon J, Yum K 3rd. Printing of anisotropic hydrogels with bioinspired motion. Advancement of Science, 2019, 6(2): 1800703–1800711
17. Gao Y, Gu S, Jia F, Gao G. A skin-matchable, recyclable and biofriendly strain sensor based on a hydrolyzed keratin-containing hydrogel. Journal of Materials Chemistry A, 2020, 8(45): 24175–24183
18. Correa S, Grosskopf A K, Lopez Hernandez H, Chan D, Yu A C, Stapleton L M, Appel E A. Translational applications of hydrogels. Chemical Reviews, 2021, 18(14): 11385–11457
19. Glowacki J, Mizuno S. Collagen scaffolds for tissue engineering. Biopolymers, 2008, 89(5): 338–344
20. Haque M A, Kurokawa T, Gong J P. Super tough double network hydrogels and their application as biomaterials. Polymer, 2012, 53(9): 1805–1822
21. Yue Y, Wang X, Wu Q, Han J, Jiang J. Highly recyclable and super-tough hydrogel mediated by dual-functional TiO_2 nanoparticles toward efficient photodegradation of organic water pollutants. Journal of Colloid and Interface Science, 2020, 564(5): 99–112
22. Liu Y, Sun Q, Yang X, Liang J, Wang B, Koo A, Li R, Li J, Sun X. High-performance and recyclable Al-air coin cells based on eco-friendly chitosan hydrogel membranes. ACS Applied Materials & Interfaces, 2018, 10(23): 19730–19738
23. Yuan T, Qu X, Cui X, Sun J. Self-healing and recyclable hydrogels reinforced with *in situ*-formed organic nanofibrils exhibit simultaneously enhanced mechanical strength and stretchability. ACS Applied Materials & Interfaces, 2019, 11(35): 32346–32353
24. Chamas A, Moon H, Zheng J, Qiu Y, Tabassum T, Jang J H, Abu-Omar M, Scott S L, Suh S. Degradation rates of plastics in the environment. ACS Sustainable Chemistry & Engineering, 2020, 8(9): 3494–3511
25. Delplace V, Nicolas J. Degradable vinyl polymers for biomedical applications. Nature Chemistry, 2015, 7(10): 771–784
26. Ben Cheikh A, Chuche J, Manisse N, Pommelet J C, Netsch K P, Lorencak P, Wentrup C. Synthesis of *α*-cyano carbonyl compounds by flash vacuum thermolysis of (alkylamino)methylene derivatives of meldrum's acid. Evidence for facile 1,3-shifts of alkylamino and alkylthio groups in imidoylketene intermediates. Journal of Organic Chemistry, 1991, 56(3): 970–975
27. Sweidan K, Abu-Salem Q, Al-Sheikh A, Sheikha G. Novel derivatives of 1,3-dimethyl-5-methylenebarbituric acid. Letters in Organic Chemistry, 2009, 6(8): 669–672
28. El-Zaatari B M, Ishibashi J S A, Kalow J A. Cross-linker control of vitrimer flow. Polymer Chemistry, 2020, 11(33): 5339–5345
29. Diehl K L, Kolesnichenko I V, Robotham S A, Bachman J L, Zhong Y, Brodbelt J S, Anslyn E V. Click and chemically triggered declick reactions through reversible amine and thiol coupling via a conjugate acceptor. Nature Chemistry, 2016, 8(10): 968–973
30. Meadows M K, Sun X, Kolesnichenko I V, Hinson C M, Johnson K A, Anslyn E V. Mechanistic studies of a "declick" reaction. Chemical Science (Cambridge), 2019, 10(38): 8817–8824
31. Sun X, Chwatko M, Lee D H, Bachman J L, Reuther J F, Lynd N A, Anslyn E V. Chemically triggered synthesis, remodeling, and degradation of soft materials. Journal of the American Chemical Society, 2020, 142(8): 3913–3922
32. Chang L, Wang C, Han S, Sun X, Xu F. Chemically triggered hydrogel transformations through covalent adaptable networks and applications in cell culture. ACS Macro Letters, 2021, 10(7): 901–906
33. Wu T, Liang T, Hu W, Du M, Zhang S, Zhang Y, Anslyn E V, Sun X. Chemically triggered click and declick reactions: application in synthesis and degradation of thermosetting plastics. ACS Macro Letters, 2021, 10(9): 1125–1131
34. Fang Y, Xu J, Gao F, Du X, Du Z, Cheng X, Wang H. Self-healable and recyclable polyurethane-polyaniline hydrogel toward flexible strain sensor. Composites Part B: Engineering, 2021, 219(22): 108965–108974